biomedicines

MDPI

Article

Sequential Conventional Panretinal Photocoagulation and Short-Term Macular Microvascular and Structural Changes: A Prospective OCT Angiography Study

Mustafa Salih Karatepe [1,*], Esra Akaydın Gültürk [2], Ayşe Vural Özeç [1], Haydar Erdoğan [1], Duygu Yalınbaş Yeter [3] and Erman Bozali [4]

[1] Department of Ophthalmology, Faculty of Medicine, Cumhuriyet University, 58140 Sivas, Türkiye; vural.ayse@gmail.com (A.V.Ö.); herdogan65@gmail.com (H.E.)
[2] Department of Biostatistics, Faculty of Medicine, Cumhuriyet University, 58140 Sivas, Türkiye; esra0709.eg@gmail.com
[3] Department of Ophthalmology, Bilkent City Hospital, 06800 Ankara, Türkiye; duyguyalinbas@gmail.com
[4] Department of Ophthalmology, Mersin City Hospital, 33240 Mersin, Türkiye; ermanbozali@gmail.com
* Correspondence: drdmsk@gmail.com; Tel.: +90-5530867975

Abstract

Background/Objectives: To evaluate longitudinal macular microvascular and structural changes during sequential conventional panretinal photocoagulation (PRP) in severe non-proliferative and early proliferative diabetic retinopathy. **Methods:** This prospective single-arm study included 53 eyes of 36 patients undergoing three PRP sessions four weeks apart. Optical coherence tomography angiography (OCT-A) was performed at baseline and four weeks after each session. Longitudinal changes were analyzed using hierarchical linear mixed-effects models, with additional analyses addressing multiple testing and missing final-visit measurements. **Results:** All 53 eyes completed the first three assessments, while 35 eyes yielded evaluable OCT-A measurements at the final visit. Foveal superficial capillary plexus vessel density (SCP VD) showed a statistically significant increase at T1 (+1.568 percentage points; 95% CI, 0.381–2.755; Holm-adjusted $p = 0.019$) and T2 (+2.092; 95% CI, 0.906–3.279; adjusted $p = 0.002$); however, the increase at T3 was not significant (+1.180; 95% CI, −0.187 to 2.547; adjusted $p = 0.091$). The global time effect ($p = 0.005$) remained significant after applying Benjamini–Hochberg false discovery rate correction across 16 outcomes (q = 0.019) but not after Holm correction (adjusted $p = 0.062$). Foveal, parafoveal, and perifoveal retinal thickness increased over time (overall $p < 0.001$ for all); no significant change was observed in the area of the foveal avascular zone or its perimeter. Exploratory sensitivity analyses indicated that assumptions regarding missing measurements could influence the SCP VD estimates for the final visit. **Conclusions:** Foveal SCP VD increased at intermediate visits, but a sustained increase was not established at the final visit. Retinal thickness increased throughout follow-up. These exploratory findings do not establish a causal effect of sequential PRP.

Keywords: panretinal photocoagulation; diabetic retinopathy; optical coherence tomography angiography; superficial capillary plexuses; foveal avascular zone; vessel density

Check for updates

Academic Editors: Ana Maria Dascalu and Dragos Serban

Received: 19 October 2026
Revised: 24 November 2026
Accepted: 25 November 2026
Published: 29 November 2026

Copyright: © 2026 by the authors. Licensee MDPI, Basel, Switzerland. This article is an open access article distributed under the terms and conditions of the Creative Commons Attribution (CC BY) license.

1. Introduction

Diabetic retinopathy (DR) is a major cause of visual impairment and is characterized by progressive microvascular injury, retinal nonperfusion, and, in advanced disease, neovascularization [1–3]. Panretinal photocoagulation (PRP) remains an established treatment

for proliferative DR (PDR) and is considered in selected eyes with severe nonproliferative DR (NPDR) [4]. Regression of neovascularization and improvement in visual acuity have been reported following PRP treatment of ischemic areas in eyes with PDR [5]. Although PRP reduces the risk of severe visual loss, it can also produce transient retinal changes, including increased macular thickness and visual symptoms [6–8].

The therapeutic effect of PRP has been attributed in part to reduced metabolic demand in the treated peripheral retina and improved oxygen availability to the remaining retinal tissue [6,7]. The underlying mechanism is primarily thought to be related to the destruction of photoreceptor cells, which are rich in mitochondria and have high oxygen consumption, and their replacement by glial scars with lower mitochondrial content. Changes in vascular endothelial growth factor signaling and retinal hemodynamics may also occur after treatment [8,9]. However, the direction and extent of macular microvascular changes cannot be inferred from these proposed mechanisms alone [10–13].

Optical coherence tomography angiography (OCT-A) permits noninvasive assessment of retinal capillary plexus vessel density (VD), the foveal avascular zone (FAZ), and selected choroidal parameters [14–16]. Previous studies evaluating OCT-A after PRP have yielded heterogeneous results, possibly reflecting differences in DR severity, laser protocols, scan acquisition, and follow-up duration [13,17–23].

Most available reports describe measurements before and after completion of PRP. The pattern of OCT-A changes across individual conventional PRP sessions remains less clearly characterized. We therefore prospectively assessed macular and choroidal OCT-A parameters at four-week intervals during a three-session conventional PRP course in eyes with severe NPDR or early PDR.

2. Materials and Methods

This prospective, single-arm longitudinal observational study was conducted at Sivas Cumhuriyet University Health Services Application and Research Hospital between January 2023 and June 2025. Eligible treatment-naive patients had severe NPDR or early PDR and were scheduled for conventional PRP in three sessions (T0-T2) four weeks apart. The study was approved by the Sivas Cumhuriyet University Faculty of Medicine Clinical Research Ethics Committee (No: 2022–11/06) and was conducted in accordance with the principles of the Declaration of Helsinki. Written and verbal informed consent was obtained from all patients.

DR severity was classified using Early Treatment Diabetic Retinopathy Study criteria, supported by color fundus photography and fluorescein angiography [4,24]. Exclusion criteria were high-risk PDR that can lead to vitreous hemorrhage and tractional retinal detachment, previous anti-VEGF treatment or PRP, age younger than 18 years, ocular trauma or vitrectomy, retinal vein occlusion or other retinal vascular disease, tractional fibrovascular proliferation, uveitis, optic neuropathy, glaucoma, refractive error greater than ±3 diopters, and conditions that could compromise OCT-A assessment (including significant cataract, central macular edema, subretinal fluid, and epiretinal membrane). Images with signal strength below 6/10 or poor fixation were excluded.

Age, sex, diabetes type and duration, HbA1c, systemic hypertension, lens status, best-corrected visual acuity (BCVA), intraocular pressure, and ophthalmic examination findings were recorded. Snellen BCVA was converted to logMAR. After pupil dilation and topical anesthesia, conventional PRP was performed with a 561-nm laser (Ellex Integre, Adelaide, Australia) using a panfundoscopic or SuperQuad lens. Nominal settings for all eyes consisted of a 200 μm spot size, a 200 ms exposure duration, and 200 mW of power. Laser power was occasionally adjusted according to the observed retinal burn response. The number of laser applications varied between eyes and sessions, depending on patient

cooperation and clinical assessments. OCT-A examinations were obtained immediately before each session and four weeks after the third session, at approximately 3:00 p.m. to reduce diurnal variation.

At the final visit (T3), which took place four weeks after the completion of the third and final PRP session, the treating clinician decided to initiate intravitreal treatment for certain eyes. This decision was based on the presence of clinically significant macular edema (including cystoid changes and/or subretinal fluid) as well as OCT findings such as intraretinal cystic spaces and hyperreflective foci, alongside a deterioration in visual acuity. Eyes in which image quality was compromised or artifacts were present due to macular edema, thereby precluding a reliable OCT-A assessment, were excluded from the OCT-A analysis at the final visit. For these previously untreated eyes, a regimen of monthly intravitreal bevacizumab injections for a duration of three months was planned, in accordance with national reimbursement requirements.

2.1. Data Collection

OCT-A was performed using the AngioVue RTVue XR Avanti system (Optovue, Fremont, CA, USA) and split-spectrum amplitude-decorrelation angiography. Automated 6 × 6-mm scans were used to quantify superficial capillary plexus (SCP) and deep capillary plexus (DCP) VD in the foveal (central 1 mm), parafoveal (1–3 mm), and perifoveal (3–6 mm) regions. The device-defined SCP extended from approximately 3 µm below the internal limiting membrane to 15 µm below the inner plexiform layer; the DCP extended from 15 to 70 µm below the inner plexiform layer. The software provided FAZ area, perimeter, and FD-300 (VD in a 300-µm-wide region surrounding the FAZ), together with retinal thickness and a choroidal flow-area measurement. The software-derived FAZ measurement was not separately assigned to the SCP and DCP. Subfoveal choroidal thickness was measured manually three times by one experienced examiner (MSK) and averaged.

OCT-A images were reviewed by an experienced examiner (MSK). Scans showing segmentation errors, low signal strength (<6/10), poor fixation, or motion and blink artifacts were repeated to obtain adequate image quality. Scans with prominent projection artifacts were also reacquired. The device's automated projection artifact correction was enabled for all scans. For quantitative analysis, the highest-quality scans meeting the signal strength threshold (≥6/10) and image quality criteria were selected.

2.2. Statistical Analysis

Continuous variables are presented as mean ± standard deviation (SD) or, where appropriate, median (interquartile range, IQR), and categorical variables as number (percentage). Laser spot counts across the three PRP sessions were compared using a linear mixed-effects model with session as a categorical fixed effect and random intercepts for patient and eye nested within patient; the global session effect was evaluated using a Wald chi-square test with two degrees of freedom. Longitudinal changes in OCT-A parameters were analyzed using maximum-likelihood linear mixed-effects models, with visit (T0–T3) included as a categorical fixed effect and random intercepts for patient and eye nested within patient to account for repeated measurements and inter-eye correlation. Measurements were available for 53 eyes at baseline (T0) and the first two follow-up visits (T1 and T2), whereas final-visit (T3) measurements were available for 35 eyes. All available observations were included in the primary analysis without imputation of missing data. The primary mixed-effects analysis relied on the missing-at-random (MAR) assumption.

Global time effects were evaluated using Wald chi-square tests with three degrees of freedom. Changes from baseline at each follow-up visit were reported as estimated mean differences with 95% confidence intervals, and p values were adjusted for three compar-

isons within each parameter using the Holm method. No single primary outcome was prespecified, as the study was designed to evaluate longitudinal changes across multiple OCT-A vascular and structural parameters. To address multiplicity across outcomes, Benjamini–Hochberg false discovery rate (FDR) and Holm corrections were also applied to the 16 global time-effect tests (eight vessel density, three retinal thickness, and three FAZ parameters, choriocapillaris flow area, and subfoveal choroidal thickness). Accordingly, the global time-effect analyses were interpreted as exploratory.

Sensitivity analyses included patient-cluster bootstrap percentile confidence intervals based on 5000 resamples of observed baseline-to-final-visit changes, accounting for inter-eye correlation (patients were resampled with replacement, and all eligible eyes of each sampled patient were retained). Additional linear mixed-effects analyses were performed using the first three visits in all 53 eyes and all four visits in the 35 eyes with complete follow-up. Baseline clinical characteristics and OCT-A parameters were compared between eyes with and without final-visit measurements using ordinary least-squares (OLS) regression with patient-clustered robust standard errors. These comparisons were exploratory, and no adjustment for multiple testing was applied.

To further assess the potential impact of missing final-visit measurements, an exploratory missing-not-at-random (MNAR) sensitivity analysis was performed using a delta-adjusted pattern-mixture approach. Missing T3 values were generated by adding randomly sampled T2-to-T3 changes from eyes with complete follow-up to the observed T2 measurements of eyes with missing final-visit data. Separate delta adjustments were then applied according to the reason for missingness. Uncertainty was assessed using 1500 patient-cluster bootstrap resamples to account for the correlation between fellow eyes. The resulting estimates and 95% bootstrap confidence intervals were examined across a range of hypothetical MNAR scenarios.

Changes in BCVA between baseline and the final visit were assessed in 35 eyes with available measurements at both time points. In the 11 eyes that received intravitreal treatment for macular edema, BCVA at the time of the treatment decision (T3) was retrieved from the medical records and analyzed separately. The mean change in logMAR BCVA and its 95% confidence interval were estimated using an intercept-only OLS regression with patient-clustered robust standard errors. Exploratory linear regression analyses were performed to evaluate the associations between changes in foveal, parafoveal, and perifoveal retinal thickness and changes in logMAR BCVA, using patient-clustered robust standard errors to account for inter-eye correlation.

Exploratory analyses were performed to assess the potential influence of DR severity and laser spot count on longitudinal OCT-A changes. Disease severity (severe NPDR or early PDR) and its interaction with visit were incorporated into linear mixed-effects models with random intercepts for patient and eye nested within patient. Global severity-by-visit interactions were evaluated using Wald chi-square tests with three degrees of freedom. Associations between total laser spot count and baseline-to-final-visit changes in OCT-A parameters were assessed using linear regression models adjusted for baseline values and retinopathy severity, with patient-clustered robust standard errors. Regression coefficients were expressed per 100 additional laser spots. Benjamini–Hochberg FDR correction was applied across 16 exploratory outcomes within each analysis. For selected associations, robustness was further assessed using 2500 patient-cluster bootstrap resamples and leave-one-patient-out analyses. All tests were two-sided, and adjusted p values or FDR q values below 0.05 were considered statistically significant, as applicable. For all analyses using patient-clustered robust standard errors, p values and 95% confidence intervals were based on a t reference distribution with $G - 1$ degrees of freedom, where G is the number of patient clusters. All statistical analyses were performed in Python (version 3.13; Python Software

Foundation, Wilmington, DE, USA) using the statsmodels (version 0.15.0) [25] and SciPy (version 1.18.1) [26] libraries. Linear mixed-effects models were fitted with the MixedLM function of statsmodels, with eye nested within patient specified as a variance component; OLS models with cluster-robust standard errors and the Holm and Benjamini–Hochberg corrections were also obtained with statsmodels.

3. Results

3.1. Study Population and Baseline Characteristics

All 53 eyes completed the three planned PRP sessions and underwent OCT-A assessment at time points T0, T1, and T2 (17 patients contributed two eyes and 19 contributed one). At the final visit (T3), which took place 12 weeks after baseline, macular edema requiring intravitreal treatment was detected in 11 eyes. For these eyes, OCT-A measurements from the final visit could either not be obtained or were excluded from the analysis due to poor image quality or artifacts. Additionally, 7 eyes were lost to follow-up. Consequently, evaluable OCT-A measurements at the final visit were obtained for 35 eyes (from 26 patients). The study flow diagram is presented in Figure 1.

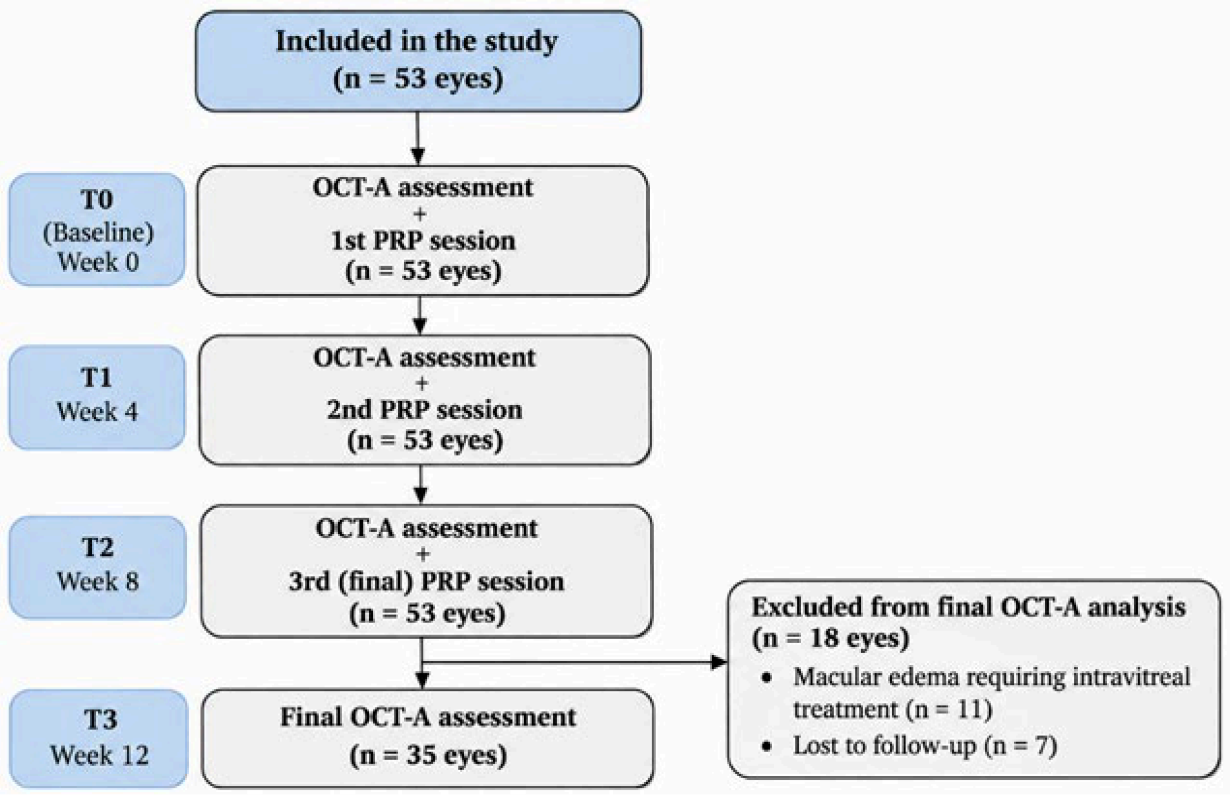


Figure 1. The study flow diagram.

Fifty-three eyes from 36 patients were analyzed (17 patients contributed two eyes and 19 contributed one). The mean age was 57.33 ± 12.19 years; 17 patients (47.2%) were female. Thirty-one eyes (58.5%) had severe NPDR and 22 (41.5%) had early PDR. Mean HbA1c was 9.26 ± 1.94%. Baseline clinical characteristics are presented in Table 1. The mean number of laser spots during the PRP sessions was 678.1 ± 265.3, 717.3 ± 300.1, and 743.3 ± 289.1, respectively, with no significant differences between sessions (Wald $\chi^2(2) = 1.90$, $p = 0.387$). The overall mean total number of laser spots for all sessions was 2138.6 ± 596.6.

Table 1. Demographic and clinical characteristics of the study population.

Parameters	Value
Patient-level characteristics (n = 36)	
Age (years)	57.33 ± 12.19
Gender, female/male, n (%)	17 (47.2)/19 (52.8)
DM type, (1/2), n (%)	2 (5.6)/34 (94.4)
Insulin/OAD use, n (%)	5 (13.9)/31 (86.1)
DM duration (years)	13.97 ± 7.24
HbA1c (%)	9.26 ± 1.94
Hypertension, n (%)	17 (47.2)
Eye-level characteristics (n = 53)	
DR severity (severe NPDR/early PDR), n (%)	31 (58.5)/22 (41.5)
Lens status (pseudophakic/phakic), n (%)	1 (1.9)/52 (98.1)

Values are presented as mean ± standard deviation or number (percentage). Percentages were calculated using 36 patients for patient-level characteristics and 53 eyes for eye-level characteristics. DM: Diabetes mellitus; OAD: Oral antidiabetic drugs; DR: Diabetic retinopathy; NPDR: Nonproliferative diabetic retinopathy; PDR: Proliferative diabetic retinopathy.

3.2. Retinal Vascular Density

Among the eight vascular density parameters, a significant global time effect was observed only for foveal SCP VD (global $p = 0.005$). Relative to baseline, foveal SCP VD increased by +1.568 percentage points at T1 (95% CI, +0.381 to +2.755; Holm-adjusted $p = 0.019$) and +2.092 percentage points at T2 (95% CI, +0.906 to +3.279; Holm-adjusted $p = 0.002$). The estimated change at T3 was +1.180 percentage points (95% CI, −0.187 to +2.547; Holm-adjusted $p = 0.091$), which was not statistically significant. No significant global time effects were detected for foveal DCP VD ($p = 0.833$), whole-image SCP VD ($p = 0.866$), whole-image DCP VD ($p = 0.885$), parafoveal SCP VD ($p = 0.261$), parafoveal DCP VD ($p = 0.872$), perifoveal SCP VD ($p = 0.987$), or perifoveal DCP VD ($p = 0.925$). None of the comparisons for these parameters (from baseline to the follow-up period) remained significant after the Holm correction was applied. Figure 2 shows the temporal changes in foveal SCP VD. After correction for multiple testing across the 16 global time-effect tests, the time effect for foveal SCP VD remained significant with Benjamini–Hochberg false discovery rate (FDR) adjustment (q = 0.019), but not with Holm adjustment (adjusted $p = 0.062$). No other vascular density parameter showed a significant global time effect after either correction (Supplementary Table S1).

3.3. Retinal Thickness

Retinal thickness increased significantly over time in all three regions (global $p < 0.001$ for each). Estimated foveal thickness increases from baseline were 8.321 µm (95% CI, 4.483–12.159), 10.679 µm (95% CI, 6.841–14.517), and 15.057 µm (95% CI, 10.617–19.498) at T1, T2, and T3, respectively. Corresponding increases in parafoveal thickness were 6.943 µm (95% CI, 4.649–9.238), 9.887 µm (95% CI, 7.592–12.181), and 12.893 µm (95% CI, 10.237–15.550). Perifoveal thickness increased by 6.698 µm (95% CI, 4.669–8.728), 9.906 µm (95% CI, 7.876–11.935), and 11.930 µm (95% CI, 9.580–14.281), respectively. All baseline-to-follow-up comparisons remained significant after Holm adjustment (all adjusted $p < 0.001$). After correction for multiple testing across the 16 global time-effect tests, the global time effects for foveal, parafoveal, and perifoveal retinal thickness remained significant under both Benjamini–Hochberg FDR and Holm adjustments (Supplementary Table S1).

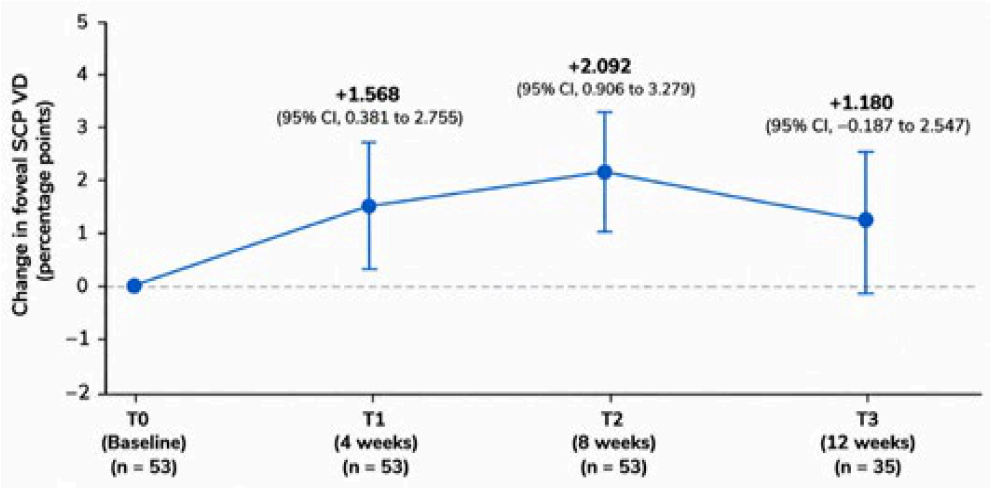


Figure 2. Temporal changes in foveal SCP VD. Points represent estimated mean changes from baseline, and error bars indicate 95% confidence intervals derived from a maximum-likelihood linear mixed-effects model with visit as a categorical fixed effect and random intercepts for patient and eye nested within patient. OCT-A measurements were available for 53 eyes at baseline (T0) and the first two follow-up visits (T1 and T2), and for 35 eyes at the final visit (T3). T1, T2, and T3 correspond to four weeks, eight weeks, and twelve weeks after the first, second, and third PRP sessions, respectively. SCP, superficial capillary plexus; VD, vessel density; PRP, panretinal photocoagulation.

3.4. FAZ, FAZ-Related Parameters, Choriocapillaris Flow, and Choroidal Thickness

There were no statistically significant global time effects for FAZ area ($p = 0.244$), FAZ perimeter ($p = 0.199$), FAZ FD-300 ($p = 0.618$), choriocapillaris flow area ($p = 0.127$), or subfoveal choroidal thickness ($p = 0.554$). For choriocapillaris flow area, the estimated change at T3 was −0.100 mm^2 (95% CI, −0.189 to −0.012); although the unadjusted p value was 0.027, the comparison did not remain significant after Holm correction (adjusted $p = 0.081$). No other baseline contrasts for these parameters were significant after adjustment. The global time effect and baseline-to-follow-up contrasts are presented in Table 2.

3.5. BCVA Changes and Their Association with Retinal Thickness

Among the 35 eyes with evaluable final-visit OCT-A measurements, mean BCVA was 0.103 ± 0.169 logMAR at baseline and 0.169 ± 0.209 logMAR at T3, with a mean paired change of +0.066 ± 0.108 logMAR (95% CI, +0.021 to +0.111; $p = 0.006$, accounting for patient-level clustering). The median paired change was +0.05 logMAR (interquartile range, 0.00 to 0.10), and four eyes (11.4%) showed a deterioration of at least 0.20 logMAR. In the 11 eyes that developed macular edema, BCVA worsened from 0.197 ± 0.179 logMAR at baseline to 0.325 ± 0.192 logMAR at the time of the treatment decision (mean change +0.127 ± 0.115 logMAR; 95% CI, +0.058 to +0.196; $p = 0.003$), with a loss of at least 0.20 logMAR in three eyes (27.3%). In exploratory analyses, changes in foveal, parafoveal, and perifoveal retinal thickness were not significantly associated with changes in logMAR BCVA (all $p > 0.05$).

3.6. Exploratory Analyses of Disease Severity and Laser Spot Count

Our study included 31 eyes with severe NPDR and 22 eyes with early-stage PDR. Final-visit OCT-A measurements were available for 21 and 14 eyes, respectively. In mixed-effects models incorporating a disease severity-by-visit interaction, no significant differences in longitudinal changes were identified between the two groups after correction for multiple testing (all FDR-adjusted q > 0.05, Supplementary Table S2).

Table 2. Longitudinal mixed-effects models.

Outcome	Global *p*	T1−T0 (95% CI); Holm-Adjusted *p*	T2−T0 (95% CI); Holm-Adjusted *p*	T3−T0 (95% CI); Holm-Adjusted *p*
Whole-image SCP VD (%)	0.866	−0.053 (−0.437 to +0.332); 1.000	−0.043 (−0.428 to +0.341); 1.000	−0.189 (−0.631 to +0.253); 1.000
Whole-image DCP VD (%)	0.885	+0.009 (−0.479 to +0.498); 1.000	+0.153 (−0.336 to +0.641); 1.000	−0.050 (−0.614 to +0.513); 1.000
Foveal SCP VD (%)	**0.005**	+1.568 (+0.381 to +2.755); **0.019**	+2.092 (+0.906 to +3.279); **0.002**	+1.180 (−0.187 to +2.547); 0.091
Foveal DCP VD (%)	0.833	−0.223 (−1.501 to +1.056); 1.000	+0.204 (−1.074 to +1.482); 1.000	−0.439 (−1.915 to +1.037); 1.000
Parafoveal SCP VD (%)	0.261	−0.138 (−0.633 to +0.358); 1.000	−0.106 (−0.601 to +0.390); 1.000	−0.566 (−1.137 to +0.006); 0.157
Parafoveal DCP VD (%)	0.872	−0.072 (−0.550 to +0.407); 1.000	+0.130 (−0.348 to +0.609); 1.000	+0.032 (−0.517 to +0.582); 1.000
Perifoveal SCP VD (%)	0.987	−0.025 (−0.442 to +0.393); 1.000	+0.043 (−0.374 to +0.461); 1.000	−0.034 (−0.515 to +0.448); 1.000
Perifoveal DCP VD (%)	0.925	−0.072 (−0.677 to +0.533); 1.000	+0.130 (−0.475 to +0.735); 1.000	+0.074 (−0.622 to +0.771); 1.000
Foveal retinal thickness (µm)	**<0.001**	+8.321 (+4.483 to +12.159); **<0.001**	+10.679 (+6.841 to +14.517); **<0.001**	+15.057 (+10.617 to +19.498); **<0.001**
Parafoveal retinal thickness (µm)	**<0.001**	+6.943 (+4.649 to +9.238); **<0.001**	+9.887 (+7.592 to +12.181); **<0.001**	+12.893 (+10.237 to +15.550); **<0.001**
Perifoveal retinal thickness (µm)	**<0.001**	+6.698 (+4.669 to +8.728); **<0.001**	+9.906 (+7.876 to +11.935); **<0.001**	+11.930 (+9.580 to +14.281); **<0.001**
FAZ area (mm^2)	0.244	−0.013 (−0.043 to +0.018); 0.842	−0.020 (−0.051 to +0.011); 0.618	+0.014 (−0.021 to +0.049); 0.842
FAZ perimeter (mm)	0.199	−0.064 (−0.181 to +0.053); 0.572	−0.097 (−0.215 to +0.020); 0.309	+0.028 (−0.106 to +0.163); 0.680
FAZ foveal density (FD-300) (%)	0.618	+0.012 (−1.021 to +1.044); 1.000	−0.603 (−1.636 to +0.429); 0.756	−0.183 (−1.371 to +1.005); 1.000
Choriocapillaris flow area (mm^2)	0.127	−0.011 (−0.088 to +0.066); 0.778	−0.043 (−0.120 to +0.034); 0.538	−0.100 (−0.189 to −0.012); 0.081
Subfoveal choroidal thickness (µm)	0.554	+0.736 (−3.867 to +5.338); 1.000	−0.434 (−5.037 to +4.169); 1.000	−3.095 (−8.424 to +2.235); 0.765

Values are estimated mean changes from baseline with 95% confidence intervals. Longitudinal changes were analyzed using maximum-likelihood linear mixed-effects models with visit as a categorical fixed effect and random intercepts for patient and eye nested within patient. Global *p* values were obtained from Wald chi-square tests with three degrees of freedom and are unadjusted. *p* values for the three follow-up comparisons with baseline were adjusted using the Holm method within each outcome. SCP, superficial capillary plexus; DCP, deep capillary plexus; VD, vessel density; FAZ, foveal avascular zone.

In exploratory analyses of the 35 eyes with final-visit measurements, total laser spot count was associated with changes in foveal DCP VD and foveal retinal thickness after adjustment for baseline measurements and retinopathy severity. For every additional 100 laser spots, the estimated change was −0.326 percentage points for foveal DCP VD and +1.223 µm for foveal retinal thickness (FDR-adjusted q = 0.049 for both). Patient-cluster bootstrap analyses yielded 95% confidence intervals of −0.549 to −0.101 and +0.502

to +2.253, respectively. Both associations remained directionally consistent in leave-one-patient-out analyses (Supplementary Table S3).

3.7. Additional Sensitivity Analyses

Additional sensitivity analyses restricted to the first three visits in all 53 eyes and to all four visits in the 35 eyes with complete follow-up showed that the global time effect for foveal SCP VD remained significant ($p = 0.001$ and $p = 0.015$, respectively). Foveal, parafoveal, and perifoveal retinal thickness also showed significant global time effects in both analyses (all $p < 0.001$). No significant global time effects were detected for the remaining vascular density measures, FAZ area or perimeter, FD-300, choriocapillaris flow area, or subfoveal choroidal thickness (all $p > 0.05$; Table 3).

Table 3. Sensitivity analyses of global time effects for all OCT-A and structural outcomes.

Outcome	First Three Visits (T0–T2, 53 Eyes) Global *p*	Complete Cases (T0–T3, 35 Eyes) Global *p*
Whole-image SCP VD (%)	0.960	0.793
Whole-image DCP VD (%)	0.819	0.600
Foveal SCP VD (%)	**0.001**	**0.015**
Foveal DCP VD (%)	0.802	0.957
Parafoveal SCP VD (%)	0.859	0.136
Parafoveal DCP VD (%)	0.607	0.853
Perifoveal SCP VD (%)	0.948	0.868
Perifoveal DCP VD (%)	0.826	0.960
Foveal retinal thickness (µm)	**<0.001**	**<0.001**
Parafoveal retinal thickness (µm)	**<0.001**	**<0.001**
Perifoveal retinal thickness (µm)	**<0.001**	**<0.001**
FAZ area (mm^2)	0.243	0.248
FAZ perimeter (mm)	0.117	0.211
FD-300 (FAZ foveal density) (%)	0.402	0.500
Choriocapillaris flow area (mm^2)	0.501	0.185
Subfoveal choroidal thickness (µm)	0.857	0.561

Longitudinal changes were assessed using maximum-likelihood linear mixed-effects models with visit as a categorical fixed effect and random intercepts for patient and eye nested within patient. Global *p* values were obtained from Wald chi-square tests (2 degrees of freedom for T0–T2 and 3 degrees of freedom for T0–T3) and are unadjusted for multiple testing. The first analysis included 159 observations (53 eyes across three visits), whereas the complete-case analysis included 140 observations (35 eyes across four visits). SCP, superficial capillary plexus; DCP, deep capillary plexus; VD, vessel density; FAZ, foveal avascular zone.

3.8. Patient-Cluster Bootstrap Sensitivity Analysis

The paired baseline-to-final-visit analysis included 35 eyes from 26 patients. In 5000 patient-cluster bootstrap resamples, the mean change in foveal SCP VD was +1.480 percentage points (95% percentile CI, 0.078–3.121). The confidence intervals for the other seven vascular density measures included zero. Mean increases in foveal, parafoveal, and perifoveal retinal thickness were 16.257 µm (95% CI, 9.999–22.559), 13.771 µm (95% CI, 9.273–18.727), and 12.771 µm (95% CI, 9.166–16.571), respectively.

The observed mean baseline-to-final changes in FAZ area, perimeter, and FAZ FD-300 were +0.013 mm^2 (95% CI, −0.040 to 0.074), +0.019 mm (95% CI, −0.172 to 0.228), and

−0.280 percentage points (95% CI, −1.573 to +1.203) respectively. Choriocapillaris flow area decreased by 0.109 mm^2 (95% CI, −0.220 to −0.009), whereas subfoveal choroidal thickness changed by −3.657 µm (95% CI, −10.407 to 3.001). The bootstrap interval for choriocapillaris flow area excluded zero, but this complete-case sensitivity finding should be considered separately from the nonsignificant global time effect and Holm-adjusted contrast in the primary longitudinal model. The analysis of changes from the observed baseline to the final status, based on the patient cohort and using the bootstrap method, is presented in Table 4.

Table 4. Patient-cluster bootstrap of observed baseline-to-final changes.

Outcome	Eyes (*n*)	Mean Change	95% Percentile CI
Whole-image SCP VD (%)	35	−0.100	−0.631 to +0.510
Whole-image DCP VD (%)	35	+0.026	−0.426 to +0.500
Foveal SCP VD (%)	35	+1.480	+0.078 to +3.121
Foveal DCP VD (%)	35	−0.383	−2.253 to +1.324
Parafoveal SCP VD (%)	35	−0.506	−1.117 to +0.109
Parafoveal DCP VD (%)	35	+0.060	−0.787 to +0.772
Perifoveal SCP VD (%)	35	+0.054	−0.483 to +0.678
Perifoveal DCP VD (%)	35	+0.071	−0.529 to +0.715
Fovea retinal thickness (µm)	35	+16.257	+9.999 to +22.559
Parafoveal retinal thickness (µm)	35	+13.771	+9.273 to +18.727
Perifoveal retinal thickness (µm)	35	+12.771	+9.166 to +16.571
FAZ area (mm^2)	35	+0.013	−0.040 to +0.074
FAZ perimeter (mm)	35	+0.019	−0.172 to +0.228
FAZ foveal density (FD-300) (%)	35	−0.280	−1.573 to +1.203
Choriocapillaris flow area (mm^2)	35	−0.109	−0.220 to −0.009
Subfoveal choroidal thickness (µm)	35	−3.657	−10.407 to +3.001

The analysis included 35 eyes from 26 patients with available measurements at both baseline and the final visit. Patient-cluster bootstrap resampling was performed with 5000 iterations, retaining all eligible eyes from each resampled patient. Mean changes represent observed paired differences, and 95% percentile confidence intervals were calculated from the bootstrap distribution. No adjustment for multiple testing was applied. These results represent a paired complete-case sensitivity analysis rather than estimates from the primary mixed-effects model. SCP, superficial capillary plexus; DCP, deep capillary plexus; VD, vessel density; FAZ, foveal avascular zone.

Exploratory baseline comparisons were performed between eyes with ($n = 35$) and without ($n = 18$) final-visit OCT-A measurements, accounting for clustering within patients. No statistically significant differences were observed in the evaluated baseline clinical characteristics, retinal vascular density parameters, retinal thickness measurements, FAZ indices, choriocapillaris flow area, or subfoveal choroidal thickness (all $p > 0.05$; Table 5).

3.9. Missing-Not-At-Random Sensitivity Analysis

Under the reference scenario without additional delta adjustments, the estimated T3–T0 change in foveal SCP VD was +1.37 percentage points (95% bootstrap CI, −0.05 to 2.90). The estimated change decreased under progressively unfavorable assumptions for missing outcomes, reaching −0.13 percentage points (95% CI, −1.85 to 1.55) in the most unfavorable scenario examined. The confidence intervals included zero in all scenarios. In

contrast, increases in foveal, parafoveal, and perifoveal retinal thickness persisted across the examined scenarios, with confidence intervals excluding zero (Table 6).

Table 5. Baseline comparison by final-visit availability.

Baseline Parameter	Available ($n = 35$)	Unavailable ($n = 18$)	Mean Difference [1]	p Value
Age (years)	55.51 ± 12.58	58.67 ± 10.56	−3.152	0.405
HbA1c (%)	9.73 ± 1.98	9.19 ± 2.09	+0.532	0.487
Diabetes duration (years)	12.83 ± 6.61	16.78 ± 7.08	−3.949	0.121
Baseline BCVA (logMAR)	0.10 ± 0.17	0.19 ± 0.18	−0.089	0.094
Whole-image SCP VD (%)	46.63 ± 1.68	46.91 ± 1.78	−0.280	0.596
Whole-image DCP VD (%)	49.65 ± 1.82	49.27 ± 1.89	+0.385	0.513
Foveal SCP VD (%)	27.85 ± 5.13	28.69 ± 5.12	−0.840	0.594
Foveal DCP VD (%)	31.37 ± 5.85	30.71 ± 6.36	+0.660	0.726
Parafoveal SCP VD (%)	45.70 ± 3.15	45.64 ± 1.89	+0.053	0.946
Parafoveal DCP VD (%)	52.09 ± 1.34	52.06 ± 1.63	+0.025	0.959
Perifoveal SCP VD (%)	46.59 ± 1.97	46.56 ± 1.90	+0.033	0.952
Perifoveal DCP VD (%)	50.87 ± 1.94	50.39 ± 2.38	+0.471	0.517
Foveal retinal thickness (µm)	259.23 ± 25.57	268.06 ± 27.18	−8.827	0.325
Parafoveal retinal thickness (µm)	322.20 ± 20.66	314.94 ± 13.51	+7.256	0.182
Perifoveal retinal thickness (µm)	292.51 ± 24.35	285.61 ± 20.13	+6.903	0.367
FAZ area (mm^2)	0.28 ± 0.10	0.30 ± 0.10	−0.016	0.636
FAZ perimeter (mm)	2.11 ± 0.40	2.16 ± 0.40	−0.047	0.725
FAZ foveal density (FD-300) (%)	44.25 ± 4.89	43.31 ± 3.21	+0.943	0.466
Choriocapillaris flow area (mm^2)	1.51 ± 0.41	1.47 ± 0.42	+0.046	0.756
Subfoveal choroidal thickness (µm)	238.54 ± 48.05	225.78 ± 53.23	+12.765	0.444

OLS regression with cluster-robust standard errors and a t reference distribution based on the number of patient clusters minus one. Values are mean ± SD unless otherwise stated. [1] Available minus unavailable. Two-sided, exploratory unadjusted p values; no multiplicity adjustment. SCP, superficial capillary plexus; DCP, deep capillary plexus; VD, vessel density; FAZ, foveal avascular zone; BCVA, best-corrected visual acuity.

Table 6. Exploratory delta-adjusted missing-not-at-random sensitivity analyses of final-visit OCT-A outcomes.

Foveal SCP VD (%)		
Delta: edema/loss to follow-up (percentage points)	**Estimated T3−T0 change (percentage points)**	**95% bootstrap CI**
0/0	+1.371	−0.051 to +2.899
−2/0	+0.957	−0.484 to +2.478
−4/0	+0.544	−1.016 to +2.095
−4/−1	+0.413	−1.160 to +2.005
−6/−2	−0.132	−1.848 to +1.554

Table 6. *Cont.*

Foveal retinal thickness (µm)		
Delta: edema/loss to follow-up (µm)	**Estimated T3−T0 change (µm)**	**95% bootstrap CI**
0/0	+13.258	+6.635 to +19.554
+10/0	+15.326	+8.934 to +21.557
+20/0	+17.395	+10.928 to +23.817
Parafoveal retinal thickness (µm)		
Delta: edema/loss to follow-up (µm)	**Estimated T3−T0 change (µm)**	**95% bootstrap CI**
0/0	+11.766	+7.096 to +16.505
+10/0	+13.866	+9.093 to +18.922
+20/0	+15.965	+10.698 to +21.407
Perifoveal retinal thickness (µm)		
Delta: edema/loss to follow-up (µm)	**Estimated T3−T0 change (µm)**	**95% bootstrap CI**
0/0	+10.947	+7.307 to +14.539
+10/0	+13.027	+9.164 to +16.812
+20/0	+15.107	+10.529 to +19.630

Final-visit measurements were available for 35 of 53 eyes; 11 eyes had missing measurements due to macular edema requiring intravitreal treatment and seven were lost to follow-up. Missing T3 values were generated by adding randomly sampled observed T2-to-T3 changes from eyes with complete follow-up to the T2 measurements of eyes with missing data. Delta adjustments were applied separately according to the reason for missingness. Deltas are hypothetical shifts in missing T3 values, not observed effects. Estimates and 95% confidence intervals are from an independent 1500-replicate patient-cluster bootstrap reanalysis; all 1500 replicates yielded results. MNAR, missing not at random; OCT-A, optical coherence tomography angiography; SCP, superficial capillary plexus; VD, vessel density; CI, confidence interval; T0, baseline; T2, second follow-up; T3, final visit.

4. Discussion

Diabetes mellitus (DM) is a chronic vascular disease that is the most common cause of retinal involvement worldwide. Microvascular complications resulting from inadequate glycemic control lead to DR and, consequently, blindness [27]. PRP is an established treatment for PDR and neovascular complications of other ischemic retinal vascular diseases, aimed at reducing the angiogenic stimulus associated with ischemic retinal tissue [28]. If ischemia is left untreated, it leads to retinal atrophy, macular edema, and neovascularization, subsequently causing vitreous hemorrhage and tractional retinal detachment, ultimately resulting in vision loss [29]. Therefore, when retinal ischemia is detected by FFA, PRP applied to the peripheral retina constitutes the cornerstone of treatment [30]. It has also been reported that neovascularization regresses and visual acuity improves following PRP treatment of ischemic areas in eyes with PDR [31]. In addition to reducing the levels of vasoproliferative factors such as VEGF released from ischemic retina, PRP may induce various structural, functional, and hemodynamic retinal changes [32,33].

To the best of our knowledge, this is the first study to evaluate the short-term effects of conventional PRP sessions on the macular and choroidal capillary plexus using sequential OCT-A imaging. In this prospective study, the foveal SCP VD exhibited a time-dependent response throughout the course of sequential conventional PRP, with statistically significant increases observed during interim follow-up examinations. Macular thickness increased throughout follow-up. In contrast, FAZ area and perimeter did not demon-

strate significant longitudinal changes after accounting for repeated measurements and fellow-eye correlation.

Previous studies evaluating retinal microvasculature after PRP in eyes with DR using OCT-A have reported variations in retinal blood flow distribution and FAZ parameters [17–22]. Faghihi et al. [17] demonstrated that in patients with severe NPDR and early PDR, there was no significant change in foveal and parafoveal SCP and DCP VD at 1 and 6 months after PRP; however, after 6 months of follow-up, the FAZ area decreased and the FAZ became more circular according to the circularity index. Although no significant differences in VD were observed, the authors suggested that this might be related to the redistribution of blood flow in the hypoperfused foveal capillary plexus [17].

In DR, changes in the FAZ area may be used as a marker for screening and treatment follow-up in diabetic patients, and enlargement of the FAZ area has been considered a poor prognostic factor [34,35]. Similarly, Sabaner et al. [20] reported in their study, which included patients with severe NPDR, that the baseline FAZ area was higher than the values measured at one and six months after PRP, suggesting that this finding might indicate ischemia control achieved with PRP. Takase et al. [36] reported that FAZ enlargement in DR is associated with capillary occlusion; however, they also showed that early retinal capillary occlusion may be transient and that significant FAZ enlargement may be reversible, at least in diabetic patients without retinopathy. Moreover, restoration of flow in the occluded macular capillary plexus has been demonstrated in both NPDR and PDR [37]. Mirshahi et al. [18] reported an increase in foveal VD three months after PRP treatment in patients with severe NPDR, while the FAZ area remained unchanged. In our study, unlike the research by Faghihi et al. [17] and Sabaner et al. [20], no significant differences were detected in the FAZ area or the region surrounding the FAZ following the PRP sessions. Furthermore, consistent with the findings of Mirshahi et al. [18], a significant overall time effect was observed in foveal SCP VD values relative to baseline.

Abdelhalim et al. [23] reported significant improvements in foveal VD and FAZ area in patients with PDR at 1 and 6 months following PRP, compared to baseline values. The increase in foveal SCP VD observed during intermediate visits in our study is consistent with their findings regarding VD; however, we did not observe a significant change in the FAZ area. Changes in retinal oxygen availability following PRP have been proposed as a potential explanation for these vascular responses [18]. Similarly, Fawzi et al. [13] suggested that PRP might be associated with a redistribution of blood flow toward the posterior pole, which could be linked to the regression of neovascular and shunt vessels. Nevertheless, these mechanisms were not directly evaluated in our study. Discrepancies in findings across OCT-A studies may reflect variations in the severity of retinopathy, laser protocols, scan acquisition, image segmentation, and the timing of follow-up. Importantly, OCT-A VD is derived from a decorrelation signal and does not directly measure volumetric blood flow. Therefore, the early increase in foveal SCP VD observed in our study should be interpreted as a longitudinal association rather than direct evidence of improved retinal oxygenation, capillary reperfusion, or the redistribution of retinal blood flow.

In the current study, following the application of the Holm correction, the estimated increase in foveal SCP VD values observed at the final visit was not found to be statistically significant in the primary mixed-effects analysis. Although the patient-cluster bootstrap analysis yielded a positive baseline-to-final change with a confidence interval excluding zero, this analysis was restricted to eyes with complete follow-up and did not account for multiple comparisons. These findings should therefore not be interpreted as evidence of a sustained increase in foveal SCP VD. Furthermore, an exploratory MNAR sensitivity analysis indicates that the estimated change at the final visit is sensitive to the assumptions

made regarding missing outcomes. Therefore, the findings from the final visit should be interpreted with caution.

In this study, the increase in retinal thickness is consistent with previous reports indicating that structural macular changes are observed following PRP [38–40]. Although PRP is used to prevent PDR, it may cause macular edema, which is considered the most common cause of decreased visual acuity in diabetic eyes [40]. While the mechanism underlying the development of macular edema after PRP remains unclear, it has been reported that clinical or subclinical macular edema may occur following PRP due to disruption of the blood–retina barrier [38,39]. However, glycemic control and underlying conditions other than DM, such as hypertensive retinopathy, also play an important role; therefore, an increase in central macular thickness after PRP does not necessarily indicate that PRP directly causes foveal thickening. This increase may also be a consequence of the natural course of the disease [19,39]. In the current study, eleven eyes required intravitreal treatment due to macular edema, and for these eyes, it was not possible to obtain analyzable OCT-A data at the final assessment. This outcome-related loss to follow-up may introduce bias into estimates concerning the final visit; furthermore, retinal edema can affect the automated segmentation process and the apparent VD. Although retinal thickness increased during follow-up, the mean deterioration in visual acuity among eyes with complete final-visit measurements was modest, and exploratory analyses did not identify a significant association between changes in retinal thickness and BCVA. Therefore, the observed changes in retinal thickness may not, in every instance, represent clinically significant macular edema. Furthermore, the exclusion of eyes with edema requiring treatment may have led to an underestimation of the overall retinal thickening present in the original cohort. Given the absence of a control group, it would not be appropriate to establish a causal link between PRP and the development of macular edema.

The finding of a significant global time effect for foveal SCP VD should be interpreted cautiously in view of the multiple vascular and structural outcomes examined. Although this association remained significant after FDR correction across outcomes, it did not withstand the more conservative Holm adjustment. Furthermore, no single primary outcome was prespecified. Accordingly, the observed changes in foveal SCP VD should be regarded as exploratory rather than confirmatory. In contrast, the increases in retinal thickness remained significant under both correction methods.

In our study, no significant overall effect of time was observed regarding the choriocapillaris flow area or subfoveal choroidal thickness. Previous studies have suggested that PRP may influence choroidal circulation through alterations in blood flow distribution or via inflammatory responses [33,41]. Variations in factors such as the level of metabolic control, the severity of retinopathy, measurement techniques, and the duration of follow-up may contribute to the heterogeneous findings reported in the literature [41–44]. Zhang et al. [45] also discussed several potential explanations for the changes in choroidal blood flow following PRP. However, our study did not directly assess choroidal blood flow volume, inflammatory activity, or autoregulatory responses. Consequently, the absence of any statistically significant change in the measured choroidal parameters neither confirms nor excludes the existence of these mechanisms.

Although severe NPDR and early PDR may differ in terms of initial microvascular damage and response to treatment, exploratory interaction analyses did not reveal significant differences in longitudinal OCT-A changes between these groups. However, the limited subgroup sizes, particularly at the final visit, constrain the ability to rule out differences related to disease severity. A higher total number of laser spots was associated with greater foveal thickening and a more negative change in the foveal DCP VD. However, the number of laser spots may not always be a reliable metric for representing the total laser energy

delivered, due to variations in treatment requirements, patient tolerance, or other clinical factors. In addition, eyes requiring more extensive laser treatment may have had more severe retinal ischemia at baseline, which could have influenced the observed associations. Therefore, the findings should be interpreted as exploratory rather than as evidence of a direct relationship between the number of laser spots and macular changes.

The strengths of this study include its prospective design, predefined imaging visits, and repeated assessments throughout sequential conventional PRP. The hierarchical mixed-effects models accounted for repeated measurements within eyes and correlations between fellow eyes of the same patient. In addition, patient-clustered bootstrap, complete-case, and missing-not-at-random sensitivity analyses were performed to assess the robustness of the findings.

A significant limitation of our study is the reduction in the number of eyes available for assessment at the final visit, from 53 to 35. Notably, the requirement for intravitreal treatment due to macular edema in 11 eyes suggests that the absence of final-visit measurements may be related to the retinal parameters under investigation. Although no significant differences in baseline characteristics were found between eyes with and without final-visit measurements, this does not rule out potential bias arising from the missing data. Consequently, an additional sensitivity analysis assuming data were "Missing Not At Random" (MNAR) was conducted, evaluating various hypothetical scenarios for eyes with missing data due to macular edema or loss to follow-up. The results indicated that the change in foveal SCP VD at the final visit could be influenced by the assumptions made regarding the missing data, whereas the increase in retinal thickness remained consistent across the scenarios examined. Nevertheless, as the true values of the missing measurements are unknown, these analyses do not entirely eliminate the possibility of selection bias. Similarly, eyes that developed macular edema showed a numerically greater BCVA decline than eyes with complete follow-up, and no BCVA data were available for the eyes lost to follow-up; therefore, the BCVA change observed in the 35 eyes may underestimate visual deterioration in the overall cohort.

Nevertheless, the study is single-arm, relatively small and limited to short-term follow-up, precluding a controlled causal estimate of PRP effects. In this study, cases of severe NPDR and early-stage PDR were analyzed together. Sabaner et al. [20] demonstrated FAZ area narrowing only in patients with NPDR who were receiving oral antidiabetic treatment and had better metabolic control. Another limitation is that the FAZ assessment software of the device used in our study provides a single FAZ value across all retinal vascular segmentation layers. By using different software, FAZ area values for the SCP and DCP can be measured separately [36]. Previous OCT-A studies have suggested that FAZ enlargement, particularly in the DCP, is common in patients with DR [36]. In addition, although the perifoveal area can be assessed using 6 × 6 mm OCT angiograms, the lower resolution in the foveal and parafoveal regions (compared to 3 × 3 mm scans), as well as challenges inherent to the OCT-A acquisition process, such as artifacts, may have influenced the data obtained. Although scans with apparent segmentation errors or prominent artifacts were reacquired, changes in retinal thickness may still have influenced automated segmentation and VD measurements. The absence of a control group in our study limits the extent to which the observed microvascular and structural changes can be directly attributed to PRP. However, since PRP is clinically indicated for the patients included in our study, it would not be ethically appropriate to discontinue or delay the treatment solely for the purpose of establishing a control group. While the sequential OCT-A measurements, performed at four-week intervals, allow for the assessment of short-term changes during the treatment process, they do not demonstrate that these changes are independent of the natural course of DR. In particular, although there was no progression in the stage of diabetic retinopathy

(DR) in the eyes throughout the study period, the relatively high HbA1c levels in the study population and the development of macular edema in some eyes during the follow-up period should be taken into account when interpreting changes in retinal thickness and OCT-A parameters. Therefore, our findings should be viewed as temporal changes observed during the course of treatment, rather than as direct causal effects of PRP. Finally, this study was conducted using conventional laser delivery systems; the results might differ if pattern-scanning laser systems were used.

In conclusion, this study observed transient changes in foveal SCP VD and an increase in retinal thickness during a series of conventional PRP sessions. No significant longitudinal changes were detected in FAZ area or perimeter. These findings should be interpreted with caution, given the missing final OCT-A measurements and the absence of a control group. Further prospective, controlled studies are needed to comprehensively evaluate the effects of PRP on the macula and choroid in various ischemic retinopathies.

Supplementary Materials: The following supporting information can be downloaded at: https://www.mdpi.com/article/10.3390/biomedicines14122789/s1, Supplementary Table S1. Multiplicity-adjusted global time effects across OCT-A outcomes; Supplementary Table S2. Exploratory associations of disease severity with longitudinal OCT-A changes; Supplementary Table S3. Exploratory associations of total laser spot count with longitudinal OCT-A changes.

Author Contributions: Conception: M.S.K., E.A.G., A.V.Ö., H.E., D.Y.Y. and E.B. Design: M.S.K., E.A.G., A.V.Ö. and H.E. Data collection: M.S.K., A.V.Ö., H.E., D.Y.Y. and E.B. Analysis/Interpretation: M.S.K. and E.A.G. Literature review: M.S.K., A.V.Ö. and H.E. Writer: M.S.K. and H.E. All authors have read and agreed to the published version of the manuscript.

Funding: The authors did not receive any specific direct financial support for the research, conduct of the study, or the writing and/or publication of the findings of this article. The general ophthalmological examination infrastructure was supported by CÜBAP (project no. T-2023-993).

Institutional Review Board Statement: The study was approved by the local ethics committee of Sivas Cumhuriyet University Faculty of Medicine Clinical Research Ethics Committee on 15 November 2022 with the number 2022-11/06 and adhered to the tenets outlined in the Declaration of Helsinki.

Informed Consent Statement: Informed consent for participation was obtained from all subjects involved in the study.

Data Availability Statement: The raw data supporting the conclusions of this article will be made available by the authors on request.

Acknowledgments: The authors acknowledge the support provided by the Sivas Cumhuriyet University Scientific Research Projects Coordination Unit (CÜBAP) for the general ophthalmological examination infrastructure, under the Research Infrastructure Support and Development Project (project number T-2023-993).

Conflicts of Interest: The authors declare no conflict of interest.

References

1. Xu, Y.; Wang, L.; He, J.; Bi, Y.; Li, M.; Wang, T.; Wang, L.; Jiang, Y.; Dai, M.; Lu, J.; et al. Prevalence and control of diabetes in Chinese adults. *JAMA* **2013**, *310*, 948–959. [CrossRef] [PubMed]
2. Klein, R.; Lee, K.E.; Knudtson, M.D.; Gangnon, R.E.; Klein, B.E. Changes in visual impairment prevalence by period of diagnosis of diabetes: The Wisconsin Epidemiologic Study of Diabetic Retinopathy. *Ophthalmology* **2009**, *116*, 1937–1942. [CrossRef] [PubMed]
3. Antonetti, D.A.; Klein, R.; Gardner, T.W. Diabetic retinopathy. *N. Engl. J. Med.* **2012**, *366*, 1227–1239. [PubMed]
4. Early Treatment Diabetic Retinopathy Study Research Group. Early photocoagulation for diabetic retinopathy: ETDRS report number 9. *Ophthalmology* **1991**, *98*, 766–785. [PubMed]
5. Feng, H.E.; Weihong, Y.U.; Dong, F. Observation of retinal neovascularization using optical coherence tomography angiography after panretinal photocoagulation for proliferative diabetic retinopathy. *BMC Ophthalmol.* **2021**, *21*, 252. [CrossRef] [PubMed]

6. Flaxel, C.; Bradle, J.; Acott, T.; Samples, J.R. Retinal pigment epithelium produces matrix metalloproteinases after laser treatment. *Retina* **2007**, *27*, 629–634. [CrossRef] [PubMed]
7. Stefánsson, E. The therapeutic effects of retinal laser treatment and vitrectomy. A theory based on oxygen and vascular physiology. *Acta Ophthalmol. Scand.* **2001**, *79*, 435–440. [CrossRef] [PubMed]
8. Moriarty, A.P.; Spalton, D.J.; Shilling, J.S.; Ffytche, T.J.; Bulsara, M. Breakdown of the blood-aqueous barrier after argon laser panretinal photocoagulation for proliferative diabetic retinopathy. *Ophthalmology* **1996**, *103*, 833–838. [CrossRef] [PubMed]
9. Mansour, A.M.; Bynoe, L.A.; Welch, J.C.; Pesavento, R.; Mahendradas, P.; Ziemssen, F.; Pai, S.A. Retinal vascular events after intravitreal bevacizumab. *Acta Ophthalmol.* **2010**, *88*, 730–735. [CrossRef] [PubMed]
10. Mendivil, A.; Cuartero, V. Ocular blood flow velocities in patients with proliferative diabetic retinopathy after scatter photocoagulation. Two years of follow-up. *Retina* **1996**, *16*, 222–227. [PubMed]
11. Song, Y.; Tani, T.; Omae, T.; Ishibazawa, A.; Yoshioka, T.; Takahashi, K. Retinal blood flow reduction after panretinal photocoagulation in Type 2 diabetes mellitus: Doppler optical coherence tomography flowmeter pilot study. *PLoS ONE* **2018**, *13*, e0207288. [CrossRef] [PubMed]
12. Yamada, Y.; Suzuma, K.; Onizuka, N.; Uematsu, M.; Mohamed, Y.H.; Kitaoka, T. Evaluation of retinal blood flow before and after panretinal photocoagulation using pattern scan laser for diabetic retinopathy. *Curr. Eye Res.* **2017**, *42*, 1707–1712. [CrossRef] [PubMed]
13. Fawzi, A.A.; Fayed, A.E.; Linsenmeier, R.A.; Gao, J.; Yu, F. Improved Macular Capillary Flow on Optical Coherence Tomography Angiography After Panretinal Photocoagulation for Proliferative Diabetic Retinopathy. *Am. J. Ophthalmol.* **2019**, *206*, 217–227. [CrossRef] [PubMed]
14. Balaratnasingam, C.; Inoue, M.; Ahn, S.; McCann, J.; Dhrami-Gavazi, E.; Yannuzzi, L.A.; Freund, K.B. Visual Acuity Is Correlated with the Area of the Foveal Avascular Zone in Diabetic Retinopathy and Retinal Vein Occlusion. *Ophthalmology* **2016**, *123*, 2352–2367. [CrossRef] [PubMed]
15. Karatepe, M.S.; Erol, Y.Ö. Optical coherence tomography angiography evaluation of retinal and choriocapillaris changes after pars plana vitrectomy for macula-off rhegmatogenous retinal detachment: Perfluoropropane versus silicone oil tamponade. *BMC Ophthalmol.* **2026**, *26*, 232. [CrossRef] [PubMed]
16. Hwang, T.S.; Gao, S.S.; Liu, L.; Lauer, A.K.; Bailey, S.T.; Flaxel, C.J.; Wilson, D.J.; Huang, D.; Jia, Y. Automated Quantification of Capillary Nonperfusion Using Optical Coherence Tomography Angiography in Diabetic Retinopathy. *JAMA Ophthalmol.* **2016**, *134*, 367–373. [CrossRef] [PubMed]
17. Faghihi, H.; Riazi-Esfahani, H.; Khodabande, A.; Khalili Pour, E.; Mirshahi, A.; Ghassemi, F.; Mirshahi, R.; Khojasteh, H.; Bazvand, F.; Hashemi, A.; et al. Effect of panretinal photocoagulation on macular vasculature using optical coherence tomography angiography. *Eur. J. Ophthalmol.* **2021**, *31*, 1877–1884. [CrossRef] [PubMed]
18. Mirshahi, A.; Ghassemi, F.; Fadakar, K.; Mirshahi, R.; Bazvand, F.; Riazi-Esfahani, H. Effects of panretinal photocoagulation on retinal vasculature and foveal avascular zone in diabetic retinopathy using optical coherence tomography angiography: A pilot study. *J. Curr. Ophthalmol.* **2019**, *31*, 287–291. [CrossRef] [PubMed]
19. Zhao, T.; Chen, Y.; Liu, D.; Stewart, J.M. Optical Coherence Tomography Angiography Assessment of Macular Choriocapillaris and Choroid Following Panretinal Photocoagulation in a Diverse Population with Advanced Diabetic Retinopathy. *Asia Pac. J. Ophthalmol.* **2020**, *10*, 203–207. [CrossRef] [PubMed]
20. Sabaner, M.C.; Dogan, M.; Akdogan, M.; Şimşek, M. Panretinal laser photocoagulation decreases large foveal avascular zone area in non-proliferative diabetic retinopathy: A prospective OCTA study. *Photodiagnosis Photodyn. Ther.* **2021**, *34*, 102298. [CrossRef] [PubMed]
21. Acar, O.P.A.; Onur, I.U. Effect of panretinal photocoagulation on retina and choroid in diabetic retinopathy: An optical coherence tomography angiography study. *Photodiagnosis Photodyn. Ther.* **2022**, *40*, 103166. [CrossRef] [PubMed]
22. Sariyildiz, C.; Çiloğlu, E.; Yetkin, E. Quantification of macular perfusion following panretinal photocoagulation for diabetic retinopathy: An optical coherence tomography angiography study. *Photodiagnosis Photodyn. Ther.* **2023**, *41*, 103233. [CrossRef] [PubMed]
23. Abdelhalim, A.S.; Abdelkader, M. Macular vessel density before and after panretinal photocoagulation in patients with proliferative diabetic retinopathy. *Int. J. Retin. Vitr.* **2022**, *8*, 21. [CrossRef] [PubMed]
24. Early Treatment Diabetic Retinopathy Study Research Group. Grading diabetic retinopathy from stereoscopic color fundus photographs–an extension of the modified Airlie House classification: ETDRS report number 10. *Ophthalmology* **1991**, *98*, 786–806. [PubMed]
25. Seabold, S.; Perktold, J. Statsmodels: Econometric and statistical modeling with Python. In *Proceedings of the 9th Python in Science Conference, Austin, TX, USA, 28 June–3 July 2010*; SciPy: Austin, TX, USA, 2010; pp. 92–96.
26. Virtanen, P.; Gommers, R.; Oliphant, T.E.; Haberland, M.; Reddy, T.; Cournapeau, D.; Burovski, E.; Peterson, P.; Weckesser, W.; Bright, J.; et al. SciPy 1.0: Fundamental algorithms for scientific computing in Python. *Nat. Methods* **2020**, *17*, 261–272. Erratum in *Nat. Methods* **2020**, *17*, 352. [CrossRef] [PubMed]

27. Cheloni, R.; Gandolfi, S.A.; Signorelli, C.; Odone, A. Global prevalence of diabetic retinopathy: Protocol for a systematic review and meta-analysis. *BMJ Open* **2019**, *9*, e022188. [CrossRef] [PubMed]
28. Brown, D.M.; Ou, W.C.; Wong, T.P.; Kim, R.Y.; Croft, D.E.; Wykoff, C.C. Targeted Retinal Photocoagulation for Diabetic Macular Edema with Peripheral Retinal Nonperfusion: Three-Year Randomized DAVE Trial. *Ophthalmology* **2018**, *125*, 683–690. [PubMed]
29. Russell, J.F.; Al-Khersan, H.; Shi, Y.; Scott, N.L.; Hinkle, J.W.; Fan, K.C.; Lyu, C.; Feuer, W.J.; Gregori, G.; Rosenfeld, P.J. Retinal Nonperfusion in Proliferative Diabetic Retinopathy Before and After Panretinal Photocoagulation Assessed by Widefield OCT Angiography. *Am. J. Ophthalmol.* **2020**, *213*, 177–185. [CrossRef] [PubMed]
30. Tan, C.S.; Chew, M.C.; Lim, L.W.; Sadda, S.R. Advances in retinal imaging for diabetic retinopathy and diabetic macular edema. *Indian J. Ophthalmol.* **2016**, *64*, 76–83. [CrossRef] [PubMed]
31. The Diabetic Retinopathy Study Research Group. Photocoagulation treatment of proliferative diabetic retinopathy: The second report of diabetic retinopathy study findings. *Ophthalmology* **1978**, *85*, 82–106. [CrossRef] [PubMed]
32. Pekel, G.; Ağladıoğlu, K.; Acer, S.; Yağcı, R.; Kaşıkçı, A. Evaluation of ocular and periocular elasticity after panretinal photocoagulation: An ultrasonic elastography study. *Curr. Eye Res.* **2015**, *40*, 332–337. [CrossRef] [PubMed]
33. Zhu, Y.; Zhang, T.; Wang, K.; Xu, G.; Huang, X. Changes in choroidal thickness after panretinal photocoagulation in patients with type 2 diabetes. *Retina* **2015**, *35*, 695–703. [CrossRef] [PubMed]
34. Krawitz, B.D.; Mo, S.; Geyman, L.S.; Agemy, S.A.; Scripsema, N.K.; Garcia, P.M.; Chui, T.Y.P.; Rosen, R.B. Acircularity index and axis ratio of the foveal avascular zone in diabetic eyes and healthy controls measured by optical coherence tomography angiography. *Vis. Res.* **2017**, *139*, 177–186. [CrossRef] [PubMed]
35. Freiberg, F.J.; Pfau, M.; Wons, J.; Wirth, M.A.; Becker, M.D.; Michels, S. Optical coherence tomography angiography of the foveal avascular zone in diabetic retinopathy. *Graefe's Arch. Clin. Exp. Ophthalmol.* **2016**, *254*, 1051–1058. [CrossRef] [PubMed]
36. Takase, N.; Nozaki, M.; Kato, A.; Ozeki, H.; Yoshida, M.; Ogura, Y. Enlargement of Foveal Avascular Zone in Diabetic Eyes Evaluated by En Face Optical Coherence Tomography Angiography. *Retina* **2015**, *35*, 2377–2383. [CrossRef] [PubMed]
37. Yamana, Y.; Oka, Y.; Ohnishi, Y.; Ishibashi, T.; Inoguchi, T. Reflow of obstructed capillaries in the maculae of humans with diabetic retinopathy, observed by fluorescein angiography. *Br. J. Ophthalmol.* **1988**, *72*, 660–665. [CrossRef] [PubMed]
38. Lee, S.B.; Yun, Y.J.; Kim, S.H.; Kim, J.Y. Changes in macular thickness after panretinal photocoagulation in patients with severe diabetic retinopathy and no macular edema. *Retina* **2010**, *30*, 756–760. [CrossRef] [PubMed]
39. Soman, M.; Ganekal, S.; Nair, U.; Nair, K. Effect of panretinal photocoagulation on macular morphology and thickness in eyes with proliferative diabetic retinopathy without clinically significant macular edema. *Clin. Ophthalmol.* **2012**, *6*, 2013–2017. [CrossRef] [PubMed]
40. Shimura, M.; Yasuda, K.; Nakazawa, T.; Tamai, M. Visual dysfunction after panretinal photocoagulation in patients with severe diabetic retinopathy and good vision. *Am. J. Ophthalmol.* **2005**, *140*, 8–15. [CrossRef] [PubMed]
41. Takahashi, A.; Nagaoka, T.; Sato, E.; Yoshida, A. Effect of panretinal photocoagulation on choroidal circulation in the foveal region in patients with severe diabetic retinopathy. *Br. J. Ophthalmol.* **2008**, *92*, 1369–1373. [CrossRef] [PubMed]
42. Augsten, R.; Königsdörffer, E.; Schweitzer, D.; Strobel, J. Nonproliferative diabetic retinopathy-reflection spectra of the macula before and after laser photocoagulation. *Ophthalmologica* **1998**, *212*, 105–111. [CrossRef] [PubMed]
43. Conti, F.F.; Qin, V.L.; Rodrigues, E.B.; Sharma, S. Choriocapillaris and retinal vascular plexus density of diabetic eyes using split-spectrum amplitude decorrelation spectral-domain optical coherence tomography angiography. *Br. J. Ophthalmol.* **2019**, *103*, 452–456. [CrossRef] [PubMed]
44. Wang, J.C.; Laíns, I.; Providência, J.; Armstrong, G.W.; Santos, A.R.; Gil, P.; Gil, J.; Talcott, K.E.; Marques, J.H.; Figueira, J.; et al. Diabetic Choroidopathy: Choroidal Vascular Density and Volume in Diabetic Retinopathy with Swept-Source Optical Coherence Tomography. *Am. J. Ophthalmol.* **2017**, *184*, 75–83. [CrossRef] [PubMed]
45. Zhang, Z.; Meng, X.; Wu, Z.; Zou, W.; Zhang, J.; Zhu, D.; Chen, T.; Zhang, Q. Changes in Choroidal Thickness After Panretinal Photocoagulation for Diabetic Retinopathy: A 12-Week Longitudinal Study. *Investig. Ophthalmol. Vis. Sci.* **2015**, *56*, 2631–2638. [CrossRef] [PubMed]

Disclaimer/Publisher's Note: The statements, opinions and data contained in all publications are solely those of the individual author(s) and contributor(s) and not of MDPI and/or the editor(s). MDPI and/or the editor(s) disclaim responsibility for any injury to people or property resulting from any ideas, methods, instructions or products referred to in the content.